Simulation of Texture Induced Elastic Anisotropy

T. Böhlke & A. Bertram
Otto-von-Guericke University, Institute of Mechanics
Postfach 4120, 39106 Magdeburg, Germany

Abstract

The texture induced elastic anisotropy of polycrystalline copper is studied for different finite deformation paths. As a homogenization technique, the TAYLOR model is used, which is a first-order theory and incorporates only a volume-fraction representation of microstructure. In order to identify the anisotropy of the macroscopic elastic behaviour, approximations of the macroscopic strain energy density corresponding to different symmetry groups are determined and compared.

Introduction

Since single crystalline copper exhibits a significant degree of elastic anisotropy, the polycrystalline elastic properties can be affected by the crystallographic texture in an amount that has to be taken into account for engineering applications [5, 13, 19]. The crystallographic texture evolution of materials with high and intermediate stacking fault energy (e.g. pure copper) can be determined by the TAYLOR model within a first-order accuracy [12]. In the present paper the evolution of the elastic properties of polycrystalline copper undergoing large inelastic deformations is numerically studied for three finite deformation modes using the full-constraint TAYLOR model.

The elastic law on the microscale, i.e. within the grains, is derived from the assumption that the elastic behaviour is not affected by inelastic deformations [2, 3]. The simulations are restricted to proportional deformation processes, and so, only isotropic hardening models [8, 15] are considered. The hardening parameters are taken from WU et al. [20].

For a given texture there are different methods to determine the corresponding elastic properties of the aggregate (see, e.g., [10]). Simple assessments are those suggested by VOIGT and REUSS [17, 18]. The advantage of these approaches is that both represent bounds of the strain energy density of the real material [9, 16]. Their disadvantage is that these estimations are the more inaccurate the higher the degree of elastic anisotropy on the microscale is. Alternative estimations, only based on one-point statistics, are the arithmetic mean of the bounds mentioned above [5, 9] and the geometric mean of the microscopic elasticity tensors [1, 14]. Both approximations are closer to experimental results than the aforementioned bounds. Higher-order approximations based on two-point statistics [11, 16] are not applicable within the TAYLOR model.

On the macroscopic scale material symmetries determined by experiments or simulations generally exist only in some approximate sense, because the microstructure induces deviations from the behaviour described by classical point-groups. For metals the elastic behaviour can be linearized within elastic ranges. Therefore, a forth-order tensor is sufficient for the description of the mechanical properties within some elastic range. In order to identify the anisotropy, the forth-order elasticity tensor given by the homogenization technique can be approximated by forth-order tensors corresponding to distinct symmetry groups. If an approximation is sufficient within a prescribed tolerance, the anisotropy can be considered as identified.

Numerical Example

The volume averages Ξ^V and Π^R of the local stiffness and compliance tensors can be decomposed into an isotropic and an anisotropic part as follows [4]

$$\Xi^V = \Xi^{VI} + \| \Xi^C - \Xi^{VI} \| \Delta, \qquad \Pi^R = \Pi^{RI} + \| \Pi^C - \Pi^{RI} \| \Delta. \tag{1}$$

Ξ^{VI} and Π^{RI} are the isotropic elasticity tensors in the cases of uniform strain and stress fields [9]. Ξ^C and Π^C represent the single crystalline elasticity tensors. $\| \cdot \|$ denotes the FROBENIUS-norm. For uniform polycrystals consisting of cubic single crystals, the tensor Δ depends only on the orientation distribution in the aggregate and is given by

$$\Delta = \frac{\sqrt{30}}{30} \left(\mathbf{I} \otimes \mathbf{I} + 2\mathbf{I}^S - \frac{5}{V} \int_V \sum_{i=1}^{3} \mathbf{g}_i \otimes \mathbf{g}_i \otimes \mathbf{g}_i \otimes \mathbf{g}_i \, dV \right), \tag{2}$$

$\mathbf{g}_i$ being the local lattice vectors, $\mathbf{I}$ the second-order identity tensor, and $\mathbf{I}^S$ the symmetric forth-order identity tensor. According to eqn. (1), the distance between the isotropic and generally anisotropic averages is influenced on the one hand by the degree of anisotropy of the single crystals through $\| \Xi^C - \Xi^{VI} \| = \sqrt{30} \left(2\Xi_{1212} - (\Xi_{1111} - \Xi_{1122}) \right) / 5$, and on the other hand by the orientation distribution in form of the tensor Δ. The norm $\| \Delta \|$ is equal to one for a single orientation, equal to zero for a uniform orientation distribution, and in the interval $(0, 1)$ otherwise. Since $\| \Delta \|$ is dimensionless, it can be interpreted as a material independent measure for the anisotropy of the aggregate within the class of polycrystals consisting of cubic single crystals.

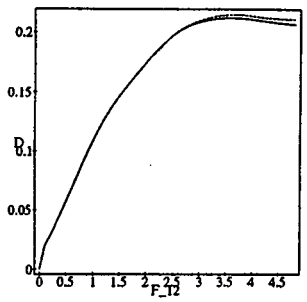

Figure 1: $D = \| \Delta \|$ vs F_{12} for simple shear and different hardening laws, H1: (–), H2: (- -).

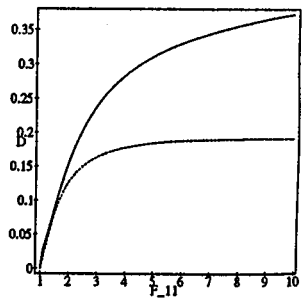

Figure 2: $D = \| \Delta \|$ vs F_{11} for plane strain compression (–) and uniaxial drawing (- -) based on H1.

In this paper the texture induced elastic anisotropy is investigated by simulating a plane strain compression, a drawing, and a simple shear deformation. In Fig. 1 the norm of Δ is shown for the simple shear deformation. The curves determined from a calculation with 1000 modified random orientations [4] and two hardening laws indicate that the predictions of both hardening models are almost the same. H1 and H2 stand for the models used in [8] and [15], respectively. For shear numbers larger than $F_{12} \approx 5$ the results depend strongly on the parameters in both the flow and the hardening rule ($\mathbf{F}$ denotes the deformation gradient).

The norm of Δ is shown in Fig. 2 for the plane strain compression and the drawing deformation. In the former case no saturation of anisotropy is observed in the range $F_{11} \in [0, 10]$, in the latter the magnitude of Δ is stationary in the range $F_{11} \in [6, 10]$, and so are the components of Ξ^V.

YOUNGs modulus predicted by Ξ^V due to a plane strain compression deformation with a thickness reduction of 90% as a function of the orientation $\{\varphi, \theta\}$ is plotted in Fig. 3. The angles $\{\varphi = 0, \theta = \pi/2\}$, $\{\varphi = \pi/2, \theta = \pi/2\}$, and $\{\theta = 0\}$ correspond to the rolling (RD), normal (ND), and transverse direction (TD), respectively. The modulus is normalized by the value predicted by the isotropic bound. In rolling and transverse direction the modulus is increased up to 15%. The maximal decrease of 20% occurs in direction $\{\varphi = 0, \theta = \pi/4\}$.

The approximation Ξ^A of the elasticity tensor, e.g. Ξ^V, is determined from the condition that Ξ^A has a certain symmetry group and minimizes the FROBENIUS norm of $\Delta\Xi := \Xi^V - \Xi^A$. If there is an exact solution of $\| \Delta\Xi \| = 0$ the identification problem is equivalent to that posed and solved in [6]. In order to solve the optimization problem $\| \Delta\Xi \| \rightarrow \min$ for a given Ξ^V, a direct search polytope algorithm [7] has been used. The standard representations of Ξ^{VA} for different symmetry classes can be easily used, if $\| \Delta\Xi \|$ is parameterized in form of

$$\| \Xi^V_{ijkl} - Q_{im} Q_{jn} Q_{ko} Q_{lp} \Xi^{VA}_{mnop} \| \rightarrow \min,$$

where Ξ^{VA}_{mnop} are the components of Ξ^{VA} with respect to the symmetry axes of the material. The Q_{ij} represent a proper orthogonal matrix describing the rotation from a reference coordinate system to the system of symmetry axes mentioned above.

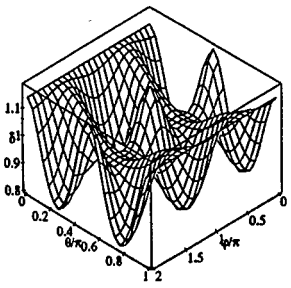

Figure 3: YOUNGs modulus $\delta = E^V / E^{VI}$.

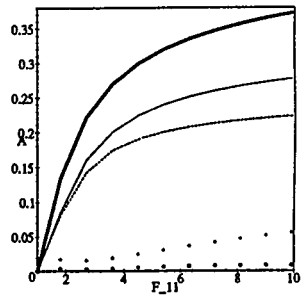

Figure 4: $A = \| \Delta\Xi^* \|$ vs F_{11} for plane strain compression.

In Fig. 4, the norm of $\Delta\Xi^* := (\Xi^V - \Xi^{VA}) / \| \Xi^C - \Xi^{VI} \|$ is shown for the plane strain compression deformation and approximations Ξ^{VA} having different symmetry groups ((-): isotropy, (-): cubic system. (- -): transverse isotropy and hexagonal systems, (+): tetragonal systems, (o): orthotropic and monoclinic system). The approximation with an orthotropic symmetry leads to a significant reduction of $\| \Delta\Xi^* \|$, which indicates that Ξ^V possesses an orthotropic symmetry within an acceptable tolerance in the modelling.

Fourth International Conference on Constitutive Laws for Engineering Materials
July 27-30, 1999

CONFERENCE PAPERS

R. C. Picu and E. Krempl, Editors

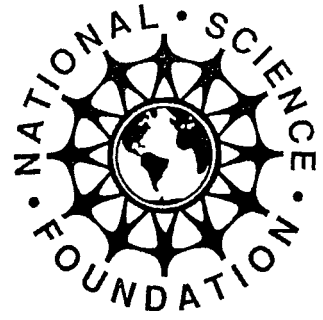

RENSSELAER POLYTECHNIC INSTITUTE
TROY, NEW YORK, USA